DIRECT NUMERICAL SIMULATION OF TURBULENT TAYLOR-COUETTE FLOWS

J.D. LI
School of the Built Environment, Victoria University of Technology,
PO Box 14428, MCMC, Melbourne, 8001, AUSTRALIA

ABSTRACT

Turbulent Taylor-Couette flows between two cylinders with the inner cylinder rotating are simulated using Direct Numerical Simulation (DNS) at a radius ratio of 0.67 and at two Reynolds numbers to investigate the Reynolds number effects on the flow. It is found that the results are consistent with the experimental results at the same radius ratio. Particular attention is given to the turbulent structures of the flows.

INTRODUCTION

Turbulent flows between concentric long cylinders with one or both cylinders rotating have been studied first by Taylor (1935). Since then many experimental works have been conducted (Barcilon et al. 1979; Koschmieder, 1979; Nakamura et al., 1981; Smith & Townsend, 1982; to mention a few). Theoretically, the flow is one of the simplest turbulent shear flows. Its simplicity is comparable to that of turbulent pipe flows. In the fully developed turbulent Taylor-Couette flows, the Reynolds stresses depend only on radius, and the closure equations are all ODE. However, our understanding towards the turbulent characteristics of this flow is far less than that for unidirectional turbulent wall shear flows, such as flows in pipes and channels.

Experimentally, it has been found (Gollub & Swinney 1975; Koschmieder 1979; Barcilon et al, 1979; Smith & Townsend 1982; Kobayashi et al 1990) that with the outer cylinder stationary, the regular laminar Taylor vortex flow persist to Taylor numbers of about 400 times the critical Taylor number T_c when laminar Couette flow becomes unstable to small disturbances. This is followed by irregular motions containing well-developed toroidal eddies similar to the laminar Taylor vortex. The experimental results of Smith & Townsend (1982) using hot-wires by introducing a small axial velocity show that at low Reynolds numbers the energy carried by these toroidal eddies is high in comparison with the total turbulent energy, and decreases as the Reynolds number increases. Smith & Townsend (1982) found that for their radius ratio of 0.67, the toroidal eddies are still detectable at $Re_d = V_1 d/\nu = 100,000$. Here $V_1 = R_1\Omega$, R_1 is the radius of the inner cylinder, Ω the angular speed of the inner cylinder, $d = R_2 - R_1$, R_2 the radius of the outer cylinder, and ν the kinematic viscosity. At this Reynolds number, the Taylor number ratio is close to 2 millions. Kobayashi et al (1990) made velocity measurements in the Taylor-Couette flow of radius ratio 0.92 using wedge-typed two-port total pressure Pitot tube for time-mean velocity and using hot-wires for turbulent stresses. To prevent the Taylor vortex shift in the axial direction, Kobayashi et al. (1990) used a grid to position the vortex at the desired location. They found that at $Re_d = 63,000$, the strength of the toroidal eddies is several times stronger than that of Smith & Townsend (1982) at $Re_d = 50,000$

Numerically the Taylor-Couette flows have been studied started from 1980's. Moser, Moin & Leonard (1983) applied their spectral method code to the Taylor-Couette flow. Marcus (1984) did the Taylor-Couette flow simulation to study the wavy-vortex with one travelling wave. Coughlin & Marcus (1992) studied the modulated waves in Taylor-Couette flow. Li (1998) presented the preliminary DNS results for radius ratio of 0.5 and Taylor number ratio of 1,300. He also shows that the turbulent intensity profiles in turbulent Taylor-Couette flow are very much different from those in unidirectional turbulent wall shear flows, and explained these differences using the energy budget equations. Rudman & Blackburn (1998) simulated the turbulent Taylor-Couette flow with counter-rotating cylinders for radius ratios of 0.875 and 0.667.

In this paper, the DNS results for Taylor-Couette flows at two Taylor number ratios of 1070 and 4280 are presented for a radius ratio of 0.67. The results are compared with the experimental results, especially those of Smith & Townsend (1982) at the same radius ratio.

NUMERICAL CONSIDERATION

Figure 1 shows the schematic diagram of the flow geometry in the present DNS simulation. Here the coordinate systems are chosen as radius r, tangential θ, and axial z with the corresponding velocity components v_r, v_θ and v_z, respectively. The axial length of the sim-

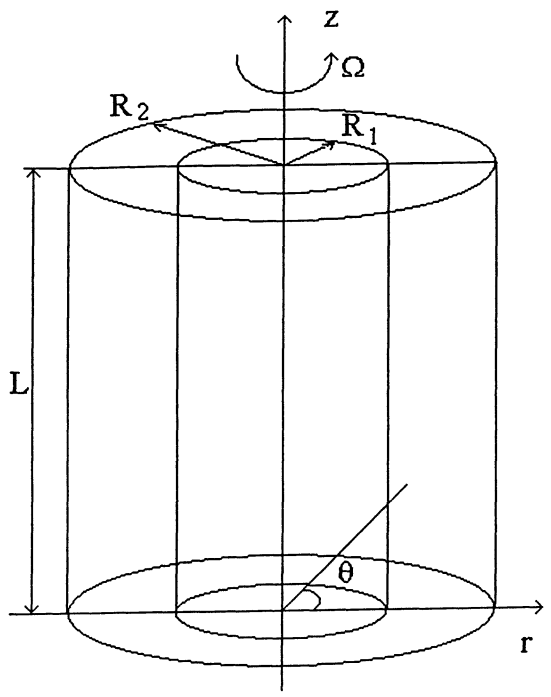

Figure 1: Schematic diagram of the flow geometry

ulation is L and the Taylor's number is defined as

$$T = \frac{2(1-\eta)}{1+\eta} Re_d^2 \tag{1}$$

Here $\eta = R_1/R_2$.

The Navier-Stokes equations are discritized according to the scheme proposed by Verstappen & Veldman (1997) as:

$$\frac{\overline{v}^* - 2\alpha v^n + (\alpha - 1/2)\overline{v}^{n-1}}{\Delta t} = -[\nabla.\overline{v}\overline{v}]^n - \frac{1}{Re_1}\nabla^2\overline{v}^{n-1} \tag{2}$$

$$\frac{(\alpha + 1/2)\overline{v}^{n+1} - \overline{v}^*}{\Delta t} = -\frac{1}{\Delta t}\nabla p^{n+1} \tag{3}$$

$$\nabla^2 p^{n+1} = \frac{1}{\Delta t}\nabla\overline{v}^* \tag{4}$$

Here $Re_1 = V_1 R_1/\nu$, $\overline{v}$ the velocity vector, n the nth time step, superscript * the intermediate time step, p the pressure fluctuations, and Δt is the time step. With $\alpha = 0.05$, the time step is estimated according to

$$\Delta t = \frac{\beta}{\frac{|v_r|}{\Delta r} + \frac{|v_\theta|}{r\Delta\theta} + \frac{|v_z|}{\Delta z} + \frac{4}{Re_1}\left(\frac{1}{\Delta r^2} + \frac{1}{r^2\Delta\theta^2} + \frac{1}{\Delta z^2}\right)} \tag{5}$$

and $\beta = 1.0$ as according to Verstappen & Veldman (1997). This time step is twice of that with $\alpha = 0$, which is the discretization scheme used in Eggles (1994) for pipe flow simulation and Li (1998) for turbulent Taylor-Couette flow simulation.

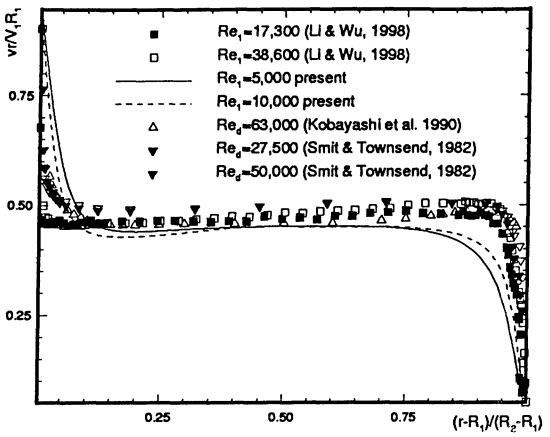

Figure 2: Normalized mean angular momentum

During simulation, periodic boundary conditions have been applied in the tangential and axial directions and Dirichlet boundary conditions were applied at the two cylinder surfaces. Initial conditions are the laminar mean velocity with imposed disturbances generated from a random number generator. The numbers of grid points used were 70 × 256 × 128 for the r, θ and z directions, respectively. Uniform grids were used in the tangential and axial directions and logarithmic grid was used in the radial direction with smaller grid spacing near the inner cylinder surface. In this study, turbulent Taylor-Couette flows at $\eta = 0.67$ were simulated with $L = 4d$, and at $Re_1 = 5{,}000$ and $10{,}000$ respectively. These correspond to Taylor number ratios of $T/T_c = 1070$ and 4280. The simulations were performed using a Pentium II computer and carried out for over 165 and 250 nondimenstional time (tV_1/R_1), respectively, for flows at the two Reynolds numbers studied.

RESULTS

Figure 2 shows the normalized mean angular momentum rV/R_1V_1 from the present DNS at $Re_1 = 5{,}000$ and $10{,}000$ together with the experimental results of Li & Wu (1998), Smith & Townsend (1982) and Kobayashi et al (1990). Both the experimental data and the DNS results show that the mean angular momentum decreases from its value at the inner cylinder surface to about half of that within a small viscous layer. Over a large proportion of the gap width between the two cylinders, the angular momentum varies only slightly, indicating the mean flow there is close to a potential flow. Near the outer cylinder surface, the angular momentum decreases rapidly to zero within a viscous layer. From the DNS data, it can be clearly seen that the effect of increasing Reynolds number is to decrease the thickness of the two viscous layers near the two cylinder surfaces.

In the central region between the two cylinders, the present mean angular momentum results from DNS are about 0.45. This is close to the experimental results of Kobayashi et al (1990), but is less than 0.5 as given by

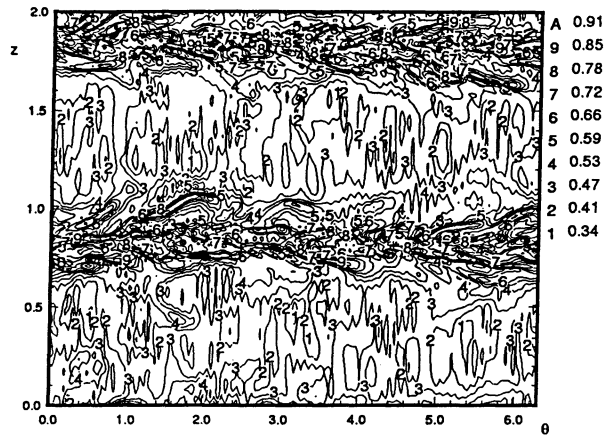

(a)

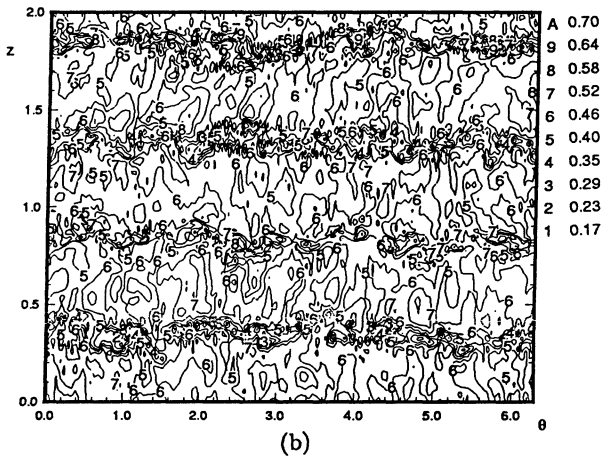

(b)

Figure 3: Contour plot of angular momentum at $Re_1 = 10,000$. (a)$r = 1.026$; (b)$r = 1.26$.

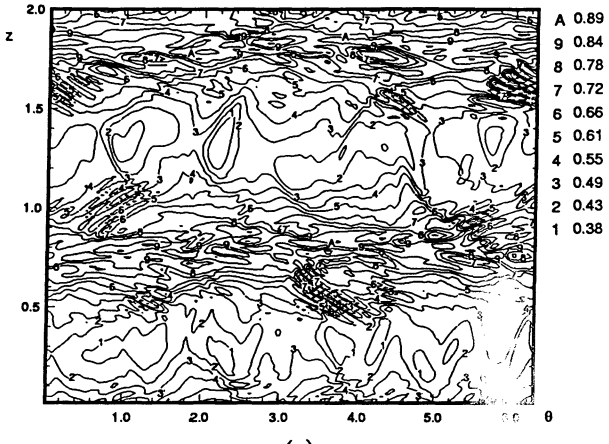

(a)

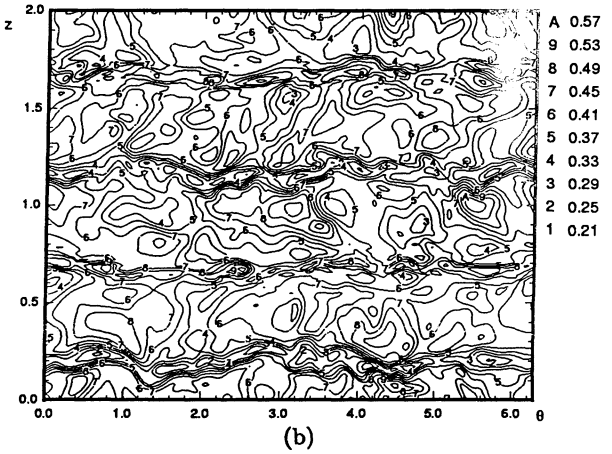

(b)

Figure 4: Contour plot of angular momentum at $Re_1 = 5,000$. (a)$r = 1.026$; (b)$r = 1.26$.

the experimental results of Smith & Townsend (1982) and Li & Wu (1998). One reason for this difference could be that in the DNS simulation, $L = 4d$ was specified. This has restricted the wavelength for the Taylor vortices to $\lambda = 2d$ (see the results given later). Koschmieder (1979) found that the wavelength for turbulent Taylor vortices is about $2.4d$ for $\eta = 0.727$ when $T > 100T_c$. This is substantially larger than the critical wavelength of laminar Taylor vortices, which is close to $\lambda = 2d$ at $\eta = 0.67$. As pointed out by Moser & Moin (1986) a chosen domain length L and the periodic boundary conditions in the axial direction will restrict the wavelength of the Taylor vortices. This will underestimate the strength and effects of the unrestricted vortices since natural vortices which are free to form with the preferred wavelength should have maximum strength. Simulation at $L = 4.8d$ is currently undertaken to investigate the wavelength effect on the mean angular momentum.

Another problem with the mean angular momentum results is that it is still slowly decreasing even after simulation time $t = 230R_1/V_1$ for $Re_1 = 10,000$For example, from $t = 230R_1/V_1$ to $t = 257R_1/V_1$, the normalized mean angular momentum in the central region has decreased from 0.456 to 0.451. The decrease is small but detectable. In the present DNS results, $t = 230R_1/V_1 \approx 48\delta/V_\tau$ for $Re_1 = 10,000$. Here δ is half of the gap width between the two cylinders. This is much longer than the $10\delta/V_\tau$ used in the channel flow simulation of Kim, Moin & Moser (1986) and the pipe flow simulation of Eggles (1994), and the $12\delta/V_\tau$ used in the curved channel flow simulation of Moser & Moin (1986). At $tV_\tau/\delta_1 \approx 10$, the normalized mean angular momentum in the present simulation in the central region is approximately 0.5, which is close to the experimental results of Smith & Townsend (1982) and Li & Wu (1998). The reason for this slow but detectable decrease in the mean angular momentum is currently not clear.

The total shear stress profiles averaged over $20R_1/V_1$ show a constant torque transport across the gap width and agree with the theoretical results that in Taylor-Couette flows, torque transport is constant

(Li, 1998). At $Re_1 = 10,000$, the normalized wall shear velocity $V_{\tau 1}/V_1$ at the inner cylinder surface is 3% less than the experimental results of Lewis & Swinney (1998) at $\eta = 0.724$. Here $V_{\tau 1} = \sqrt{\tau_{w1}/\rho}$ and τ_{w1} is the wall shear stress at the inner cylinder surface. Also it is felt that the restricted wavelength of the turbulent Taylor vortex will underestimate the wall shear velocity.

Figures 3 (a,b) show the contour plots of angular momentum vr at $Re_1 = 10,000$ and $r = 1.026$ and 1.26, respectively. The corresponding $y^+ = (r - R_1) * V_{\tau 1}/\nu$ and (Vr/V_1R_1) at these two locations are 14 (0.519) and 135 (0.451), respectively. Figure 3a shows the existence of two high angular momentum bands, one is located at $z \approx 0.8$ and the other at $z \approx 1.8$. Figure 3b shows the existence of four bands, two with high angular momentum and two with low angular momentum. The two high angular momentum bands are at the same z locations as those in figure 3a, the two low angular momentum bands are at $z \approx 0.3$ and $z \approx 1.3$. The locations of these bands depend on the initial conditions during simulation, and are the outflow and inflow jets refereed by Coughlin & Marcus (1992). The distance between these bands are the same irrespective the initial conditions.

In comparison with the numerical results of Coughlin & Marcus (1992), the outflow and inflow bands are not strongly wavy. Wereley & Lueptow (1998) conducted experiments on the spatio-temporal character of the non-wavy and wavy Taylor-Couette flow for $\eta = 0.83$ using Particle Image Velocimetry (PIV). They found that the azimuthal wave height h decreases with increasing Taylor numbers. They showed that h/d measured by the vortex center decreases from 0.65 to about 0.1 as the Taylors number increases from $4T_c$ to $140T_c$ without abating. The Taylor numbers of 1070 and 4280 in the present simulation are much higher than those investigated by Werely & Lueptow (1998), and it is clear from figures 3 (a, b) that the large scale wavy azimuthal vortices are not obvious, and it seems that they have been succeeded by small scale turbulent motions near the high and low angular momentum bands.

It can also be seen from figure 3a that narrow long streaks similar to that observed in unidirectional turbulent wall shear flows exist near the outflow jets. The average length of the streaks is about $500\nu/V_{\tau 1}$. These streaks are not perpendicular to the z axis and the angles between the streaks and the line normal to the z axis are small. However such long streaks are not obvious in figure 3b. This shows that the long streaks shown in figure 3a are near wall turbulent structures. Both figures 3a and 3b show that in turbulent Taylor-Couette flows at the present Reynolds numbers investigated, small scale turbulent motions mainly exist near the inflow and outflow jets. In the center of the Taylor vortex, the flow is relatively quiet. Because the convection of the flow by the Taylor vortex, it is expected the turbulent motions near the inflow and outflow jets will be able to mix with the near laminar flow near the centers of the Taylor vortex. The fact that only weak turbulent motions exist near the vortex center shows that the Taylor vortex has a stabilizing effects on turbulent motions. This stabilizing effect can be understood by

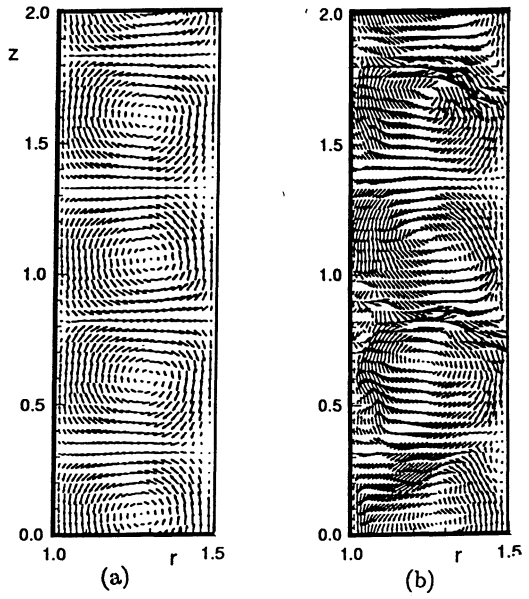

Figure 5: Velocity vector plot over r-z plan for $Re_1 = 10,000$. (a)the azimuthal average; (b)at $\theta = \pi/2$

using the Rayleigh criteria. The circulation around the Taylor vortex increases from the center of the vortex and becomes maximum midway between the neighboring vortexes. It is expected that at very high Reynolds numbers, the turbulent mixing will be strong and the stabilizing effect at the vortex centers will be small and turbulent flow in the central region between the two cylinders will be homogeneous in the axial direction.

Figures 4(a,b) show the similar plots as those of figures 3(a,b) at $Re_1 = 5,000$ and at $r = 1.026$ and 1.26. From figures 3 and 4, the effects of increasing Reynolds number on the turbulent structures can be clearly seen. It can be seen from figures 3 and 4 that as the Reynolds number increases, there are more small scale motions near the outflow and inflow jets. In comparison with figure 3a, figure 4a shows no apparent long streaks near the outflow jet, this indicates that the long streaks in figure 3a are also a result of increasing Reynolds number. In comparison with figure 3b, figure 4b shows that the inflow jets at $Re_1 = 5,000$ may be wavy.

It is clear from figures 3 and 4 that small scale turbulent motions exist and are concentrated near the outflow and inflow jets. Figures 3 and 4 show that the turbulent Taylor vortices are ring shaped. Because of these, azimuthal average can be taken. This azimuthal average is equivalent to the conditional average taken by Smith & Townsend (1982) using hot-wires by introducing a small axial velocity. Figure 5a shows the averaged velocity-vector plot over the $r - z$ plane at $Re_1 = 10,000$. Here the regular Taylor vortex can be seen. Figure 5a shows that two vortex pairs exist between the two cylinders, and the wavelength of the Taylor vortex is $2d$. Because $L = 4d$ was specified in the simulation, the wavelength of the Taylor vortex is fixed. A close look at the vortex structures in figure 5a

shows that they are different from those of laminar Taylor vortices and are the toroidal eddies studied by Smith & Townsend (1982) and Kobayashi et al (1990). Figure 5b shows the velocity vector plot at one azimuthal location at $Re_1 = 10,000$. In comparison with laminar Taylor vortex, turbulent Taylor vortices are not regular and there are small scale eddies in them, especially in regions where the local outflow jets exist. Coughlin & Marcus (1992), from their investigation of modulated waves in Taylor-Couette flow, concluded that the existence of jets between adjacent Taylor vortices produces further instability. This is distinct from the centrifugal instability which results in the generation of Taylor vortex. The fact that the present simulation shows the small scale motions concentrated near the inflow and outflow bands supports the conclusions of Coughlin & Marcus (1992).

Figures 6(a,b) show the contour plot of angular momentum vr over the same $\theta = \pi/2$ plane for $Re_1 = 5,000$ and $10,000$. Here the outflow and inflow jets can be clearly seen. It can be seen from figure 6 that these jets are strong and angular momentum in the jets has been preserved over a long distance. In general, it can be seen from figure 6 that the inflow jets can penetrate closer to the inner cylinder surface than those of outflow jets to the outer cylinder surface. Comparing figures 6(a,b) also shows that at high Reynolds numbers, the distance for the jets to preserve their angular momentum is shorter than that at low Reynolds number. This is because that the higher the Reynolds number, the stronger is the turbulent mixing. It can be seen from figure 6a that the scales for the turbulent motions near the outflow jet region and near the inner cylinder surface are smaller than those near the inflow jet region and near the outer cylinder surface. Using the analogy with unidirectional turbulent wall shear flows, it can be assumed that the length scales of the small scale turbulent motions near the wall are proportional to the viscous length scale ν/V_τ. For turbulent Taylor-Couette flows, the wall shear velocity $V_{\tau 2}$ at the outer cylinder surface is related to that of inner cylinder surface by

$$V_{\tau 2} = R_2 V_{\tau 1}/R_1 \qquad (6)$$

due to the constant torque transport. This shows that the viscous length scale at the outer cylinder surface is larger than that at the inner cylinder surface by a factor of R_2/R_1. Because of this difference in viscous length scales near the two cylinder surfaces, it is possible that the outflow jets become unstable to small disturbances at smaller Reynolds number than that for the inflow jets. Thus it is expected that the flow near the inner cylinder surface and near the outflow jets is more turbulent than that near the outer flow cylinder and near the inflow jets for a given Re_1.

DISCUSSION AND CONCLUSIONS

Direct numerical simulation has been performed for turbulent Taylor-Couette flows with $\eta = 0.67$ and at $Re_1 = 5,000$ and $10,000$. The mean angular momentum results are consistent with the experimental results of Kobayashi et al. (1990) The contour plots of angular momentum show that strong inflow and out flow jets exists. The results show that the inflow and outflow

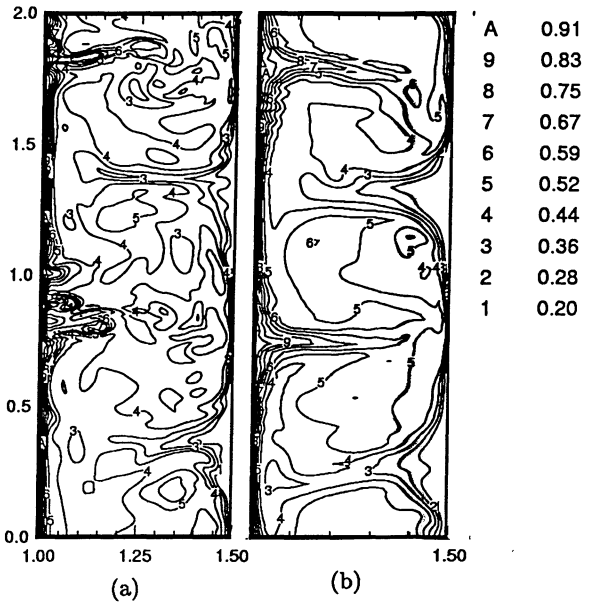

Figure 6: Contour plot of angular momentum vr at $\theta = \pi/2$. (a) $Re_1 = 10,000$; (b) $Re_1 = 5,000$.

jets are not the wavy vortex investigated by Coughlin & Marcus (1992), especially at high Reynolds number, and small scale turbulence exists near the jets. As Reynolds number increases, the distance over which the inflow and outflow jets preserve their angular momentum becomes shorter. It is also shown that the flow near the inner cylinder surface and near the outflow jets is more turbulent than that near the outer cylinder and inflow jets. Long narrow streaks are fond in the outflow jet region and near the inner cylinder surface at high Reynolds number. These streaks are similar in shape and length to the streaks observed in near wall regions of the unidirectional turbulent wall shear flows.

REFERENCES

Barcilon, A., Brindley, J. Lessen, M. & Mobbs, F.R. 1979 *J. Fluid Mech.* **94**, 453-463.

Coughlin, K. T. & Marcus, P. S. 1992, *J. Fluid Mech.* **234**, 19-46.

Eggels, KJ. G. M. 1994 *Direct and Large Eddy Simulation of Turbulent Flow in a Cylindrical Pipe Geometry,* Ph.D thesis, Delft University, the Netherlands.

Gollub, J. P. & Swinney, H. L. 1975, *Phys. Review Lett.* **35**, 927.

Kim, J., Moin, P. & Moser, R. D. *J. Fluid Mech.* **177**, 133-166.

Kobayashi, M., Maekawa, H., Takano, T. & Yamada, Y. 1990 *JSME International Journal, Series II,* **33**, *No.3,* 436-445.

Koschmieder, E. L. 1979 *J. Fluid Mech.* **93**, 515.

Lewis, G. S. & Swinney, H. L. 1998 *Phys. Rev. E.*

Li, J. D. 1998 *Proceedings of the 13th Australasian Fluid Mechanics Conference,* Monash University, Melbourne, Australia, Editors Thompson & Hourigan, **1**, 167-170.

Li, J. D. & Wu, J. 1998 *Proceedings of the 13th Aus-*

tralasian Fluid Mechanics Conference, Monash University, Melbourne, Australia, Editors Thompson & Hourigan, **2**, 765-768.
Li, J. D. & Wu, J. 1999 *submitted for publication.*
Marcus, P. S. 1984 *J. Fluid Mech.* **146**, 65-113.
Moser, R. T. & Moin, P. 1987 *J. Fluid Mech.* **175**, 479-510.
Moser, R. D., Moin, P. & Leonard, A. 1983 *J. Comp. Phys.* **12**, 524.
Nakamura, I., Yamashita, S., Watanabe, T. & Sawaki, Y. 1981 In *Proc. 3rd Symp. on Turbulent Flows*, University of California, Davis.
Rudman, J. & Blackburn, H. M. 1998 *Proceedings of the 13th Australasian Fluid Mechanics Conference*, Monash University, Melbourne, Australia, Editors Thompson & Hourigan, **1**, 163-166.
Smith, G. P. & Townsend, A. A. 1982 *J. Fluid Mech.* **123**, 187-217.
Taylor, G. I. 1935 *Proc. R. Soc. Lond.* A**151**, 494-512.
Verstappen, R.W.C.P. & Veldman, A.E.P., 1997 *J. Eng. Math.*
Wereley, S. T. & Lueptow, R. M. 1998 *J. Fluid Mech.*, **364**, 59-80.